

# **Assisted spray pyrolysis production and characterisation of ZnO nanoparticles with narrow size distribution**

**S. Turner<sup>1\*</sup>, S. M. F. Tavernier<sup>2</sup>, G. Huyberegts<sup>3</sup>, E. Biermans<sup>1</sup>, S. Bals<sup>1</sup>, K. J. Batenburg<sup>4</sup> and G. Van Tendeloo<sup>1</sup>**

1. EMAT, University of Antwerp, Groenenborgerlaan 171, B-2020 Antwerp, Belgium
2. Karel de Grote University College – dept. of Applied Engineering and Technology, Salesianenlaan 30, B-2660 Hoboken, Belgium
3. Umicore Group R&D, Kasteelstraat 7, B-2250 Olen, Belgium
4. Vision Lab, University of Antwerp, Groenenborgerlaan 171, B-2020 Antwerp, Belgium

\*Corresponding author:      Stuart Turner  
Email: Stuart.turner@ua.ac.be  
Tel: +32-3-2653572

## **ABSTRACT**

Nano-sized ZnO particles with a narrow size distribution and high crystallinity were prepared from aqueous solutions with high concentrations of Zn<sup>2+</sup> containing salts and citric acid in a conventional spray pyrolysis setup. Structure, morphology and size of the produced material were compared to ZnO material produced by simple spray pyrolysis of zinc nitrates in the same experimental setup.

Using transmission electron microscopy and electron tomography it has been shown that citric acid assisted spray pyrolysed material is made up of micron sized secondary particles comprising a shell of lightly agglomerated, monocrystalline primary ZnO nanoparticles with sizes in the 20-30 nm range, separable by a simple ultrasonic treatment step.

## **KEY WORDS**

ZnO, nanoparticles, citric acid assisted spray pyrolysis, (HR)TEM, Electron Tomography

## INTRODUCTION

In recent years, zinc oxide (ZnO) has promoted itself as a particularly interesting metal oxide material because of its unique properties (ZnO is an n-type semi-conductor) in combination with an exceptional chemical stability. Possible and proven fields of application include gas sensors, varistors, solar cells, cosmetics, photo catalysis and pharmaceuticals [11, 14, 15]. Many of these applications call for nano-sized material (nanoparticles) as the increased surface to volume ratio and specific morphology of nanostructures is known to influence the properties of the ZnO material [14]. In the past, ZnO nanomaterials have been synthesized using various methods: thermal decomposition, sol-gel, precipitation, forced hydrolysis and spray based (aerosol) production methods [3, 8, 13, 17]. *Spray pyrolysis* is one of these aerosol-based production methods and is of particular interest as it is a single-step method, and is capable of producing homogenous material with a narrow size distribution, uniform shape and controlled purity in large quantities. Through accurate control of the precursor chemistry, chemical uniformity and stoichiometric composition of multi-component metals or metal-oxides can easily be achieved using this technique [7].

Two drawbacks of the spray pyrolysis based production of nanoparticles are (1) the “one drop - one particle” reaction mechanism [10] and (2) the presence of material of low crystallinity or amorphous material due to short reactor residence times [7]. The “one-drop - one particle” mechanism usually leads to the formation of hollow or porous structures, with average particle sizes in the micron range (dependant on the initial generated droplet size). The formation of these hollow structures is caused by the fast evaporation and reaction rates inherent to spray pyrolysis, and the consequent lack of time for solute diffusion and particle densification [7].

A possible answer to the “one drop - one particle” reaction mechanism was found in the salt-assisted spray pyrolysis production [16], which was also used for ZnO nanoparticle production [12]. Although this production scheme allows several nano-sized particles to be formed from one single droplet, the necessity of an extra post-production washing step and production at high salt and low metal concentrations make this method unattractive for industrial applications. A second and more industrially viable answer to the “one drop

– one particle” and the low crystallinity problem was found with the introduction of polymeric precursors (originally introduced to achieve a better morphology control) [6]. With a correct control of the concentrations of these compounds (such as citric acid or ethylene glycol) and of the metal-ion containing salts, spherical structures in the micron size range made up of loosely agglomerated nanoparticles could be formed [9].

In this work, we describe the production of ZnO nanoparticles by citric acid (CA) assisted spray pyrolysis at high precursor concentration. The influence of the citric acid addition on the final product is studied by producing material from a citric acid carrying solution, and carefully comparing the produced material to ZnO produced by conventional spray pyrolysis at comparable experimental conditions. X-ray diffraction and electron microscopy are used to characterize both materials. Conventional bright field transmission electron microscopy (TEM) allows an accurate determination of the particle size distribution whereas high resolution TEM (HRTEM) and electron diffraction (ED) are used to determine the morphology and crystallinity of the nano material. Finally, advanced electron tomography shows the distribution of the loosely agglomerated nanoparticles in the shell of the spherical ZnO structures.

## EXPERIMENTAL

### *Particle production*

A schematic diagram of the spray pyrolysis setup used in this study is shown in figure 1. The system consists of a collision-type droplet generator, a two-step reactor furnace (400 mm - 1000 mm) with a quartz tube reactor (diameter 30 mm) and flat-filter particle collector. The process flow was obtained using a vacuum pump. The carrier gas flow in the production setup was kept constant at 1.0 l/min. All material was pyrolysed at a reactor temperature of 600°C for both furnaces. The material was collected on a flat Teflon-coated filter (Sartorius). No post-production treatment step was carried out on the samples.

The citric acid assisted ZnO material was produced from a precursor solution of 1.5 M  $\text{Zn}(\text{NO}_3)_2 \cdot 6\text{H}_2\text{O}$  (Acros Organics) and 1.5M citric acid (Acros Organics). Conventional spray pyrolysed ZnO material was produced from a precursor solution of 1.5 M  $\text{Zn}(\text{NO}_3)_2 \cdot 6\text{H}_2\text{O}$ .

### *Powder Characterisation*

X-ray diffraction experiments were carried out on a Philips PW3020 diffractometer over a scan range of angle  $2\theta = 20^\circ$  to angle  $2\theta = 80^\circ$  using steps of  $0.01^\circ$  and an acquisition time per step of 2 seconds.

Transmission electron microscopy, high resolution transmission electron microscopy and electron diffraction experiments were performed on a Philips CM30 operated at 300kV, and a JEOL 4000EX operated at 400 kV. Average secondary particle size and average primary nanoparticle size of the citric acid assisted material were measured from the obtained electron micrographs assuming a spherical morphology of the particles, providing number-based averages.

Electron tomography experiments were carried out on a JEOL 3000F TEM-STEM microscope equipped with a Fischione tomography holder with tilt range  $+80$  to  $-80$  degrees and operated at 300kV. The tilt series for tomographic reconstruction was acquired in high angle annular dark field scanning transmission electron microscopy (HAADF-STEM) mode to avoid unwanted diffraction contrast.

The powders were prepared for TEM by dispersing in methanol, and placing several drops of the dispersion onto a holey carbon grid.

### RESULTS and DISCUSSION

SEM images of spray pyrolysis produced ZnO material are shown in figure 2. In figure 2a, conventionally produced material is displayed. The spherical secondary particles have an approximate average particle size of 0.7 micron. The structures appear to be dense, and in some cases they show a collapsed or buckled shape. In figure 2b, the citric acid (CA) assisted spray pyrolysed material is displayed. As was the case for the conventional spray pyrolysed material, the CA assisted secondary structures are spherical, and also have an average particle size of 0.7 micron. The spheres appear to have a thinner and smoother shell than the conventionally produced material.

The crystal structure of both materials was first investigated using X-ray diffraction. The measured XRD patterns are displayed in figure 3. Both materials show peaks corresponding to the wurtzite hexagonal crystal structure of ZnO (space group 186).

However, the conventional spray pyrolysis produced material has a lower crystalline content and also shows peaks corresponding to not fully reacted precursor material which are not visible in the CA-assisted sample. The peaks in the CA-assisted sample fully correspond to wurtzite ZnO and show a clear broadening as a result of the small primary particle size in this sample. As a first indication, the particle size was derived from the peak broadening in the XRD pattern for the CA-assisted sample. Using the Scherrer equation on the broadening of the 100 peak, an average primary particle size of 18 nm was obtained.

To image the primary nanoparticles building up the secondary structures, TEM was used. In figure 4, the conventionally produced material is shown. Figure 4a shows a typical dense secondary structure that consists of many primary nanoparticles heavily entangled into a three dimensional structure [16]. Some non-crystalline material is still present (indicated by arrows). The wurtzite hexagonal crystal structure of the ZnO material is evidenced by the inset selected area electron diffraction (SAED) ring pattern. In figure 4b, a similar dense structure is displayed. In figure 4c, a single ZnO nanoparticle is imaged along the [001] zone axis, evidencing that some particles are single crystal, and not heavily agglomerated.

Typical CA-assisted spray pyrolysis ZnO material is shown in figure 5. The bright field TEM image of a typical CA-assisted secondary particle shows that the shell of the sphere consists of primary nanoparticles in the 20-30 nm range. The spheres in the CA assisted material appear to be less dense than the spheres produced by conventional spray pyrolysis, and the shell is far thinner. The structure does not seem to be a 3D entanglement; only the shell of the spherical structure appears to be made up of nanoparticles. The structure of the material is wurtzite ZnO, as evidenced by the inset SAED ring pattern. The small average particle size in this sample causes some broadening of the rings in the SAED pattern. Two typical nanoparticles at higher magnification are displayed in figure 5b and 5c. They are defect-free single crystals, and are not agglomerated or clustered.

Conventional TEM can only provide 2D information. In this case it is however important to have 3D information on the CA assisted sample. It is to be expected that a 3D reconstruction would show that the primary nanoparticles produced in the CA assisted

setup form the shell of the secondary spheres. A 3D reconstruction could also be used to determine the degree of agglomeration between individual particles (important for the separation possibilities of the nanoparticles). To this end, electron tomography experiments based upon a tilt series of HAADF-STEM images were carried out on the CA-assisted sample. In the HAADF-STEM imaging mode, the image contrast is proportional to the atomic number of the material that is imaged and to the thickness of the material, yielding dark vacuum and bright material. An initial reconstruction was computed using a conventional SIRT algorithm, which is commonly used for electron tomography in materials science [4, 5]. Slices through the reconstructed volume are displayed in figure 7 (top row). Although the particles can be fairly well recognized by this reconstruction algorithm, the surfaces and the boundary between the particles are not accurately reconstructed. This is due to the presence of artefacts which are difficult to avoid in a 3D reconstruction. A new and powerful reconstruction technique called discrete tomography was used to overcome these limitations. Discrete tomography exploits prior knowledge about the studied materials to obtain a better reconstruction with fewer artefacts [1, 2]. This prior knowledge includes the fact that the structure of interest consists of only a known and limited amount of compositions, each having a homogeneous density. In this case the prior knowledge used is that a pixel in the 2D projection obtained by HAADF-STEM either represents ZnO or corresponds to vacuum. The result of the discrete tomography reconstruction is displayed in figure 7 (bottom row). The slices through the reconstructed volume of the secondary particle clearly show the boundaries and surfaces of the nanoparticles and the contrast in the images is highly improved. The arrows indicate the effectiveness of the discrete algorithm: even a slight agglomeration between the particles is picked up in the reconstruction.

A 3D representation (vortex) of the same secondary structure is displayed in figure 6. Figure 6a shows an original HAADF-STEM image at zero degrees tilt. In figure 6b the discrete tomography reconstructed volume is displayed. It can be seen that the primary nanoparticles make up the shell of the secondary spherical particle. This is made clearer by slicing the reconstructed volume (slice performed through the plane indicated in figure 6b). The result is displayed in figures 6c and 6d. The ZnO can be seen to form the shell of

the secondary particles, and are only lightly agglomerated or sintered together (most of the particles are well separated in images 6c and 6d).

To obtain a detailed histogram and to test the stability of the secondary structures, the CA assisted powder was placed in an ultrasonic bath for 10 minutes. As can be seen from figure 8a, this ultrasonic treatment suffices to break down the secondary spherical structures and retain only the primary nanoparticles. A histogram obtained from the measurement of 100 nanoparticles from this type of bright field TEM images is plotted in figure 8b. The average primary particle size measured from the TEM images is 22 nm with a narrow size distribution ( $\sigma_{\lognormal} = 1.30$ ). The possibility of deagglomeration means that powders produced by CA assisted spray pyrolysis have a dual functionality. Firstly the powders can be used without deagglomeration, in processes where the secondary particle size can be exploited for easy filtration or removal of material without loss of the nano-characteristics of the powder. Secondly, the powders can easily be deagglomerated and finely dispersed using a simple ball-milling or an ultrasonic treatment step.

## CONCLUSION

Using several electron microscopy techniques we have shown that citric acid assisted spray pyrolysis is capable of producing ZnO nanoparticles with primary particle sizes within the range of 20 nm - 30 nm and a narrow size distribution at high precursor concentration and high production rate. We have shown that by using CA-assisted spray pyrolysis, the problem of “1 drop – 1 particle” production of standard spray pyrolysis can be overcome. Using electron tomography, we have shown that the primary particles are formed at the surface of the droplets, and that they form the thin shell of the secondary structures. The particles are not heavily entangled into a 3D matrix as is the case with standard spray pyrolysis produced material. This weak agglomeration in CA-assisted samples makes deagglomeration and dispersion using a simple ball-milling step or ultrasonic dispersion perfectly feasible.

## ACKNOWLEDGEMENT

The authors acknowledge support from the European Union under the Framework 6 program under a contract from an Integrated Infrastructure Initiative (Reference 026019 ESTEEM).

## SUPPORTING INFORMATION

A 3D discrete tomography reconstructed movie showing a secondary spherical structure built up of primary ZnO nanoparticles produced by CA-assisted spray pyrolysis.

## REFERENCES

- [1] Bals S., Batenburg K. J., Verbeeck J., Sijbers J., Van Tendeloo G. (2007) Quantitative Three-Dimensional Reconstruction of Catalyst Particles for Bamboo-like Carbon Nanotubes, *Nano Letters* 7: 3669-3674
- [2] Batenburg K. J., Bals S., Sijbers J., Kübel C., Kaiser U., Conrado E. A., Midgley P.A., Hernandez J.-C., Van Tendeloo G. (2008) 3D Imaging of Nanomaterials by Discrete Tomography, submitted to *Ultramicroscopy*
- [3] Dang Z.M., Fan L.Z., Zhao S.J. and Nan C.W. (2003) Preparation of nanosized ZnO and dielectric properties of composites filled with nanosized ZnO, *Materials Science and Engineering B* 99: 386–389
- [4] Gilbert P. (1972) Iterative methods for the three-dimensional reconstruction of an object from projections, *J. Theor. Biol.*, 36: 105-117
- [5] Gregor J., Benson T. (2008), Computational Analysis and Improvement of SIRT, *IEEE Trans. Medical Imaging*, 27: 918-924
- [6] Kang H.S., Kang Y.C., Park H.D. and Shul Y.G. (2003) Morphology of particle prepared by spray pyrolysis from organic precursor solution, *Materials Letters* 57: 1288-1294
- [7] Kudas T.T., Hampden-Smith M.J. (1999) *Aerosol processing of materials*, Wiley, New York
- [8] Lee J.H., Ko K.H. and Park B.O. (2003) Electrical and optical properties of ZnO transparent conducting films by the sol–gel method, *Journal of Crystal Growth* 247: 19–125
- [9] Lee K. K, Kang Y.C., Jung K. Y., Kim J.H. (2005) Preparation of nano-sized BaTiO<sub>3</sub> particle by citric-acid assisted spray pyrolysis. *Journal of Alloys and Compounds* 395: 280-285
- [10] Lenggoro I.W., Itoh Y., Lida N., Okuyama K. (2003) Control of size and morphology in NiO particles prepared by a low-pressure spray pyrolysis, *Materials Research Bulletin* 38: 1819-1827
- [11] Look D.C. (2001) Recent advances in ZnO materials and devices, *Materials Science and Engineering B* 80: 383–387
- [12] Panatarani C., Lenggoro I.W., Okuyama K. (2003) Synthesis of single crystalline ZnO nanoparticles by salt-assisted spray pyrolysis, *Journal of Nanoparticle Research* 5: 47-53



- [13] Singh P., Kumar A. and Deepak D. K. (2007) Growth and characterization of ZnO nanocrystalline thin films and nanopowder via low-cost ultrasonic spray pyrolysis, *Journal of Crystal Growth* 306: 303-310
- [14] Tian Z R, Voigt J A, Liu J, Mckenzie B, Mcdermott M J, Rodriguez M A, Konishi H. and Xu H. (2003) Complex and oriented ZnO nanostructures, *Nature Materials* 2 (12): 821-826
- [15] Wang X.D., Summers C.J., Wang Z.L. (2004) Large-Scale Hexagonal-Patterned Growth of Aligned ZnO Nanorods for Nano-optoelectronics and Nanosensor Arrays, *Nano Letters* 4: 423-426
- [16] Xia B., Lenggoro I.W., Okuyama K. (2001) Novel route to Nanoparticle Synthesis by Salt-Assisted Aerosol Decomposition, *Advanced Materials* 13: 1579-1582
- [17] Yang Y., Chen H., Zhao B. and Bao X. (2004) Size control of ZnO nanoparticles via thermal decomposition of zinc acetate coated on organic additives, *J. Cryst. Growth* 263: 447–453

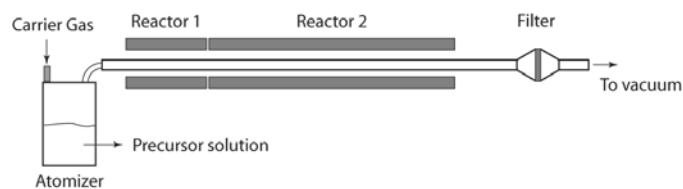


**Figure 1: Experimental nanoparticle spray-pyrolysis production setup**

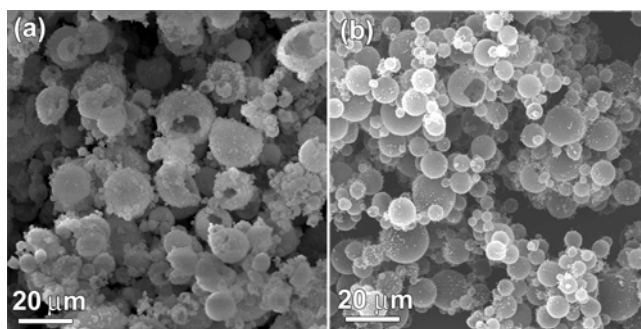


**Figure 2: SEM images of spray pyrolysis produced ZnO material; (a) Conventional spray pyrolysed material; (b) CA-assisted spray pyrolysed material; both materials consist of secondary particles in the micron size range. The particles produced with the CA method appear to have a thinner and smoother shell than the conventionally produced material. The conventionally produced material appears to be denser.**

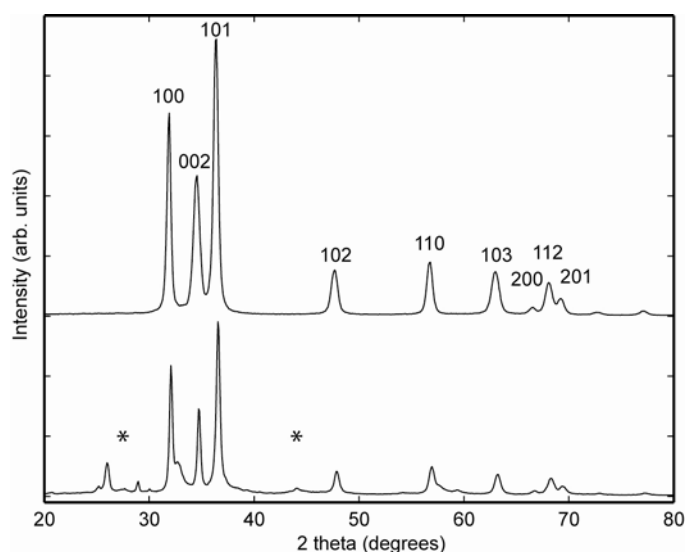


**Figure 3: XRD patterns of ZnO samples; Bottom – Conventional spray pyrolysed material. The XRD pattern shows some extra peaks (indicated by \*) corresponding to not fully reacted precursor material. Top – CA-assisted spray pyrolysed material. Only peaks corresponding to the wurtzite hexagonal ZnO crystal structure (space group 186) are present.**

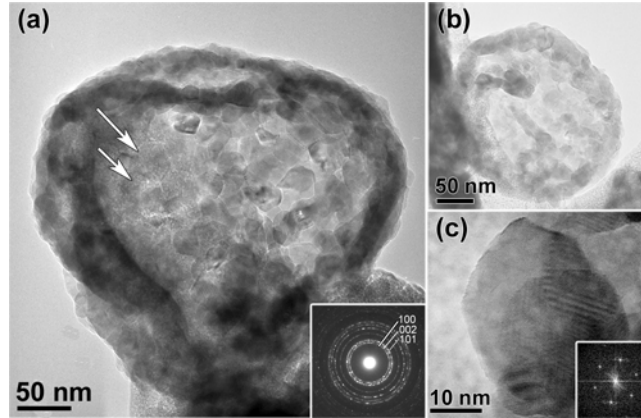


**Figure 4: Conventional spray pyrolysed ZnO material;** (a) Bright field TEM image showing the original spherical droplet shape (secondary particle size): Primary particles of 30-40 nm are visible, but all heavily agglomerated. Some non-particulate material is also present. Inset: SAED ring pattern, evidencing the wurtzite hexagonal crystal structure of the material; (b) Bright field TEM image of a secondary structure: primary nanoparticles are heavily agglomerated; (c) High resolution image of a typical ZnO nanoparticle along the [001] zone axis orientation.

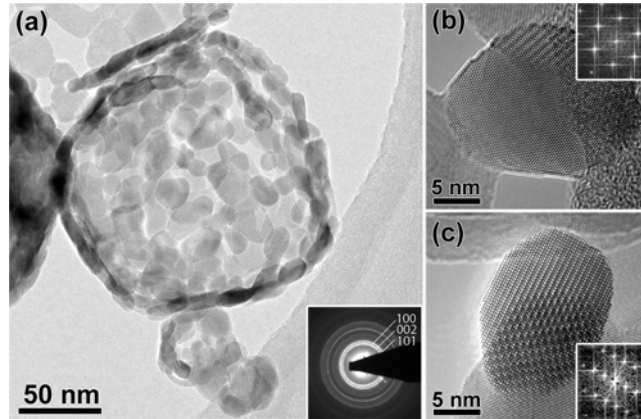


**Figure 5: Typical CA-assisted spray pyrolysis ZnO;** (a) Bright Field TEM image showing the original spherical droplet shape (secondary particle size) inset: SAED ring pattern evidencing the hexagonal wurtzite crystal structure; (b) HRTEM image of a ZnO particle along the [001] zone axis; (c) HRTEM image of a ZnO particle along the [010] zone axis. The nanoparticles are not or lightly agglomerated.

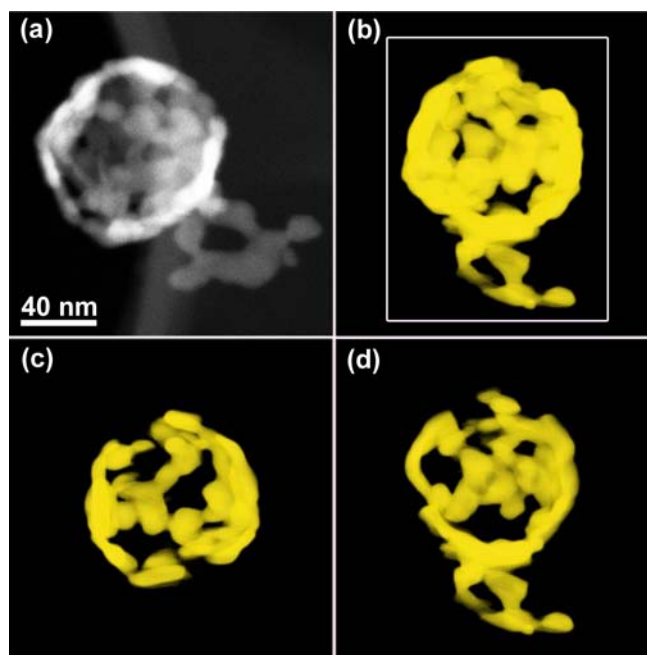


**Figure 6:** *Electron tomography on typical CA produced ZnO:* (a) HAADF-STEM image taken at zero tilt, the 3D particle structure is not apparent; (b) Tomographically reconstructed volume. The primary particles make up the shell of the secondary spherical structure; (c) & (d) Half volumes produced by clipping the reconstructed volume through the plane indicated in (b). The primary particles can clearly be observed. All particles are below 25 nm in diameter, and are only loosely (or not) agglomerated.

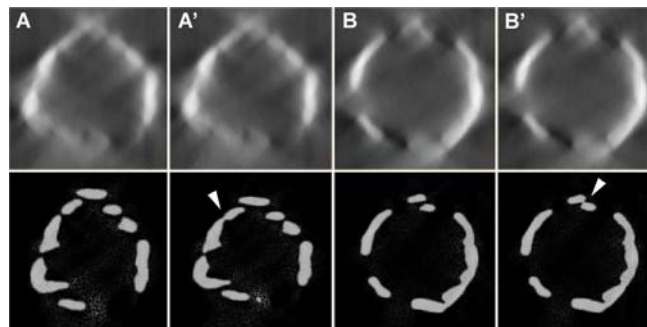


**Figure 7:** *Electron tomography orthoslices:* Top - Conventional SIRT reconstructed slices; pairs A, A' and B, B' are consecutive slices through the reconstructed volume. The lower contrast and reconstruction artefacts blur information on the particle boundaries and the degree of agglomeration. Bottom - Slices through the reconstruction based on the novel discrete tomography algorithm: the nanoparticles can be clearly made out. The arrows indicate a slight agglomeration between two nanoparticles.

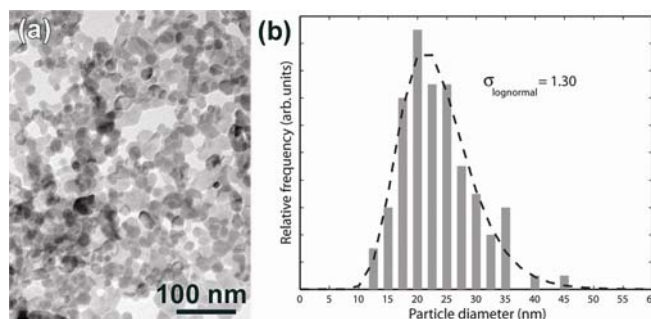


**Figure 8: Particle size distribution; (a) CA assisted sample after ultrasonic treatment; the spherical structures have broken down. (b) Nanoparticle diameter measured from 100 nanoparticles (bar chart) and fitted lognormal distribution (dashed line). The particles have an average diameter of 22 nm with a narrow particle size distribution ( $\sigma_{\text{lognormal}} = 1.30$ )**